

Phonon instabilities in uniaxially compressed fcc metals as seen in molecular dynamics simulations

Giles Kimminau,¹ Paul Erhart,² Eduardo M. Bringa,³ Bruce Remington,² and Justin S. Wark^{1,*}

¹*Department of Physics, Clarendon Laboratory, University of Oxford, Parks Road, Oxford OX1 3PU, United Kingdom*

²*Lawrence Livermore National Laboratory, Livermore, California 94550, USA*

³*CONICET and Instituto de Ciencias Básicas, Universidad Nacional de Cuyo, Mendoza CP 5500, Argentina*

(Received 5 January 2010; published 10 March 2010)

We show that the generation of stacking faults in perfect face-centered-cubic (fcc) crystals, uniaxially compressed along [001], is due to transverse-acoustic phonon instabilities. The position in reciprocal space where the instability first manifests itself is not a point of high symmetry in the Brillouin zone. This model provides a useful explanation for the magnitude of the elastic limit, in addition to the affects of box size, temperature, and compression on the time scale for the generation of stacking faults. We observe this phenomenon in both simulations that use the Lennard-Jones potential and embedded atom potentials. Not only does this work provide fundamental insight into the microscopic response of the material but it also describes certain behavior seen in previous molecular dynamics simulations of single-crystal fcc metals shock compressed along the principal axis.

DOI: [10.1103/PhysRevB.81.092102](https://doi.org/10.1103/PhysRevB.81.092102)

PACS number(s): 62.20.F-, 02.70.Ns, 61.72.Bb

When a perfect single crystal is deformed beyond its elastic limit, defects are homogeneously nucleated which allows plastic flow. This is of importance because it can be seen as the ideal strength of a material which is an upper bound of what can be obtained practically. Numerical studies of this ideal case have benefited from the advent of large-scale non-equilibrium molecular dynamics (NEMD) simulations, which allow the calculation of the motion of tens and even hundreds of millions of atoms over the course of simulation periods that can now approach of order of a nanosecond. Significant progress in understanding at the atomic level has been made in the fields of shear deformation,^{1,2} crack-tip propagation,³ and nanoindentation^{4–6} but one area where our understanding of this process has remained elusive is uniaxial shock compression. Of particular interest, and subject to a great deal of study,^{7–22} is the mechanism by which a perfect face-centered-cubic (fcc) metal, shocked to a point on the Hugoniot above its elastic limit, relieves the high shear stresses present at the shock front and approaches the hydrostatic state.

From the pioneering work of Holian and co-workers onward,⁷ the above-cited work has demonstrated that perfect fcc metals, shocked along the [001] axis, relax after the homogeneous generation of stacking faults close to the shock front, which subsequently allows the system to act in such a way as to reduce the shear stress. Despite the considerable volume of interest that this problem has generated, as yet there does not seem to be a common view as to the underlying mechanism behind the defect generation. Several ideas have been proposed previously, most of which are variations on the traditional engineering view of a critical shear stress^{12,23} and thermal activation.^{14,15} However, Clatterbuck *et al.*²⁴ reported that phonon instabilities occur in *ab initio* simulations of Al under uniaxial tension and shear, and Li *et al.*²⁵ discussed soft phonon modes leading to defects under hydrostatic tension but until now, their role in uniaxial compression has not been investigated.

In this Brief Report, we explain the fundamental mecha-

nism for stacking-fault generation in NEMD simulations of perfect fcc crystals under [001] uniaxial compression. We demonstrate that defect generation at low temperature and uniaxial compression can be described in terms of soft (unstable) phonon modes, which grow on picosecond time scales to produce stacking faults. The characteristics of these soft modes, in terms of their complex frequencies and distribution within the Brillouin Zone (BZ) as a function of compression, explains several key aspects of such NEMD simulations that have been a matter of debate for some years. We show why defect generation occurs not, as might naively be thought, simply above a critical shear stress but (as shown in Fig. 1) at a certain stress and strain. A knowledge of the time scale and means by which defects nucleate, and how this varies with temperature, could be of importance in the simulation of ramp (isentropically) compressed materials—an

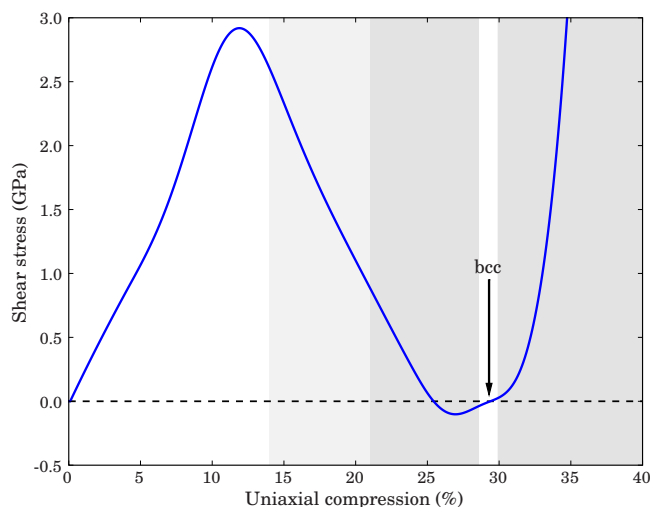


FIG. 1. (Color online) Shear stress as a function of uniaxial compression along [001] using the Cu-Mishin potential (Ref. 26) at 0 K. The shaded regions show the range of compression for which stacking faults are generated in a perfect crystal.

area of burgeoning research interest. Furthermore, the wavelength of the instabilities determines the periodicity of the defects generated, and hence influences the defect density and strength of the material. Importantly, the fact that the unstable regions are not at high-symmetry positions of the BZ further explains why certain simulation box sizes are required to observe plasticity at certain values of compression, and how the box size determines the time scale for defects to be generated. We believe this understanding of defect generation will be invaluable in the future design of NEMD simulations aimed at understanding the critical time scales required for defect generation, and how the input parameters of simulation size, temperature, and strain rate determine the plastic behavior and hence strength of the sample. We go on to consider how this model can be applied to shocks and why in simulations with small box sizes we often do not see all of the four possible $\{111\}$ slip planes activated.

The results presented here are not strongly potential dependent. We focus on simulations using the Cu potential by Mishin *et al.*,²⁶ performed with the molecular dynamics package LAMMPS,²⁷ although we have observed similar features with many other potentials that have been designed to model fcc metals. These include the Lennard-Jones potential,⁹ the Al and Ni embedded-atom method (EAM) potentials by Mishin *et al.*,²⁸ Ag EAM by Williams *et al.*,²⁹ and the Al potentials by Zope and Mishin³⁰ and Ercolessi and Adams.³¹

Figure 1 shows the instantaneous shear stress, where $\sigma_{shear} = 0.5[\sigma_{zz} - 0.5(\sigma_{xx} + \sigma_{yy})]$, as a function of uniaxial compression along $[001]$ for Cu-Mishin at 0 K. The maximum in the shear stress at 12%, with a reduction toward zero at 29.3% compression is well understood, being due to the Bain path,³² an fcc lattice compressed along $[001]$ such that the lattice parameter becomes $1/\sqrt{2}$ of its original value leads to a bcc lattice (and hence shear-free state). However, what is less clear is why uniaxial shock simulations using this potential only exhibit the generation of defects and subsequent plastic flow for uniaxial compressions above 14% (the shaded regions in the figure)—that is to say plasticity is not simply dependent on exceeding a certain stress but a certain strain. In order to answer this question, we have interrogated the stability of the lattice as a function of uniaxial compression by determining the phonon-dispersion relation over the entire BZ. The dispersion relations were calculated both by the Born-von Kármán force-constant approach,³³ and by insertion of single small-amplitude known-wavelength sinusoidal perturbations in an otherwise perfect crystal, and determining the restoring forces to calculate phonon frequency, ω for a given amplitude.

For Cu-Mishin, we indeed find that the lattice first goes unstable at 14% uniaxial compression—precisely the compression required for defects to be observed in uniaxial shock compression.¹⁷ Importantly, for compression defined to be along the z axis, the region that first goes unstable is transverse acoustic and centered along $[445]$, i.e., not at a direction of high symmetry. As the uniaxial compression is increased, the region of instability within the BZ grows. In Fig. 2, we plot the $\langle 110 \rangle$ plane of dispersion space at a uniaxial

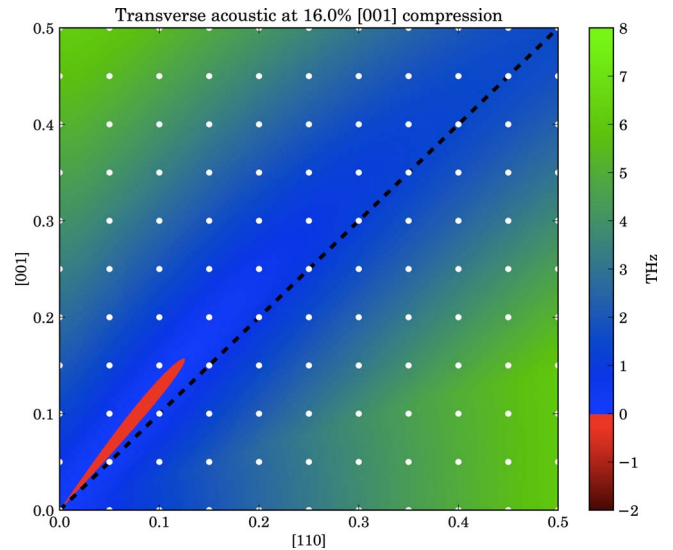


FIG. 2. (Color online) Dispersion relation for Cu-Mishin in the $\langle 110 \rangle$ plane of reciprocal space for 16% uniaxial compression along $[001]$. The color scale represents phonon frequency. The white dots indicate the phonon modes set by having a $20 \times 20 \times 20$ unit-cell box. The dashed line represents the $[111]$ transverse branch which has an e vector in the $[11\bar{2}]$ direction.

compression of 16%—just above the elastic limit. Complex values of ω are represented as negative values. We see that a volume of the BZ slightly away from the $[111]$ branch becomes unstable. The polarization vectors of these pure transverse unstable modes are as close as possible to the slip direction which is $[11\bar{2}]$. While the dispersion surface can be generated at arbitrary resolution and is independent of box size, in a particular NEMD simulation the available phonon modes are determined by the boundary conditions. Hence, for simulations of cubic samples with periodic boundary conditions (PBCs) in all three dimensions while there would always be phonon modes lying along the $[111]$ branch of dispersion space, if the box size were small, the next-nearest mode may miss the soft region altogether, and no defects would be generated, despite being above the critical compression. For example, in Fig. 2, the white dots indicate the phonon modes set by having a $20 \times 20 \times 20$ unit-cell box—note none intercept the unstable region in the BZ and Cu-Mishin uniaxially compressed to 16% within such a box responds totally elastically.

As the compression is increased, the volume of the unstable region in the BZ grows until we near a bcc structure. For Cu-Mishin, it encompasses the $[111]$ branch above 21%, and only at this point would one notice the instability within the lattice if plotting the phonon-dispersion curve along directions of high symmetry. Furthermore, at this compression even the smallest of simulation boxes will have a mode that falls within the unstable region. As compression is increased further, the volume of the unstable region eventually starts to diminish but this time toward the zone boundary rather than where it started close to the origin. In Cu-Mishin, it vanishes at 28.6% compression, just before the point of the crystal becoming bcc. If we compress the crystal further, we find that softening occurs along the $[100]$ branch indicating that

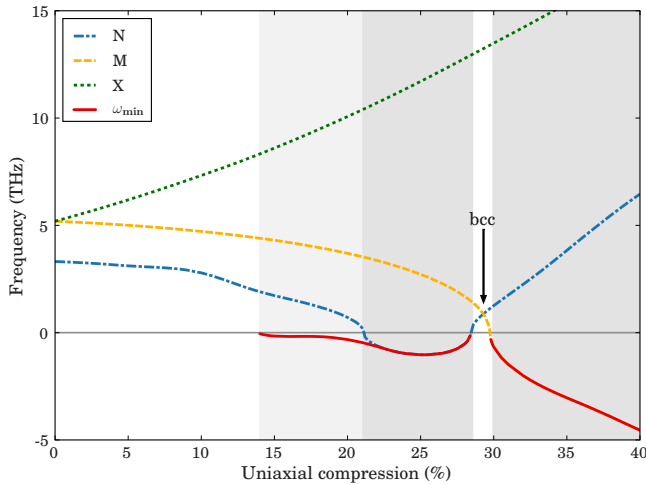


FIG. 3. (Color online) Phonon frequencies as a function of compression for high-symmetry points within the fcc primitive BZ corresponding to space group 139 ($I4/mmm$) using the Cu-Mishin potential. The unstable region does not coincide with the high-symmetry points until 21% compression.

plasticity will no longer be in the form of $\langle 111 \rangle$ stacking faults. This is illustrated in Fig. 3 which shows the phonon frequencies as a function of compression at points of high symmetry within the BZ. The N point corresponds to the zone-boundary mode at $(0.5, 0.5, 0.5)$ in the uncompressed conventional fcc cell (top right-hand corner of Fig. 2) which results in $\{111\}$ shearing, leading to stacking faults. The Γ -M direction corresponds to $[100]$ in the conventional fcc cell and likewise the Γ -X direction corresponds to $[001]$. Thus a simple phonon analysis not only indicates if the system is unstable but also the type of defects that will be generated. In systems using the Lennard-Jones potential,⁹ we also see an unstable region form just off the $[111]$ branch but this time at 16.5% uniaxial compression and continuing on beyond 34% implying that bcc is unstable.

Having demonstrated that regions of the BZ are unstable under uniaxial compression, we now consider the growth of these modes from thermal noise and the subsequent generation of stacking faults. We create an initially cubic simulation box with PBCs which we populate with atoms arranged in a perfect fcc lattice. Each atom is then assigned a random velocity from a Gaussian distribution corresponding to the desired temperature, before rescaling the entire system in the z direction to the required uniaxial compression and running the simulation under constant NVE conditions (microcanonical ensemble). The time at which defects are created after the start of the simulation, τ_c , is observed by monitoring the centrosymmetry parameter⁴ which allows us to determine when the stacking order of $\{111\}$ planes changes from the fcc order of the perfect crystal to the hcp order of a stacking fault. Previous work in shock simulations has defined nucleation to occur only once a stacking fault has reached a critical size¹⁵ but this is not relevant here because the growth of such defects is very prompt in comparison to τ_c in the examples we present.

As an illustrative example, we consider the case of a box consisting of $40 \times 40 \times 40$ unit cells of Cu-Mishin at 16%

compression. By inspecting Fig. 2, one notes that a box of $40 \times 40 \times 40$ unit cells will have double the number of modes in each dimension than those shown, and hence a mode will fall right in the middle of the unstable region with a \mathbf{q} vector of $(0.1, 0.1, 0.125)$. The level of compression dictates the dispersion landscape and the box size defines the mode locations but the temperature determines the initial-mode populations and hence the initial-mode amplitude, A_0 . The unstable modes grow exponentially until a critical amplitude is reached, A_c , in this case $\sim 0.25 \text{ \AA}$ which corresponds to $\{111\}$ planes having slipped far enough to be classed as stacking faults. Thus the time taken for the stacking faults to be generated τ_c is a function of A_0 and hence a function of temperature. For a system at 300 K, this process is almost instantaneous (~ 500 fs, comparable to the thermal equilibration time) but at 1 K, we determine τ_c to be ~ 5 ps and at 10^{-10} K, ~ 16 ps. Likewise, for a given initial temperature, the box size will also cause a variation in τ_c because it determines where within the BZ the modes are located and hence their growth rate. Obviously this model of exponential growth breaks down when anharmonicity becomes significant such as during the final stages of stacking-fault generation or at high temperature.

This behavior is of importance because it can result in a time lag for stacking-fault generation, which can be in the order of picoseconds at low temperature and the burgeoning interest in isentropic (ramp) compression. If a NEMD simulation of a ramp-compressed material is being performed at low temperature, one could easily ramp compress through an unstable region too quickly and miss out on the defect generation that might well be present in a room-temperature simulation.

While the simulations so far have been for cubic boxes with three PBCs, we can also start to see how these phonon instabilities might manifest in shock simulations. The situation in shock simulations is obviously more complicated due to the lack of a PBC in the shock direction, the heating from rapid compression and the general inhomogeneity along the shock direction. Although extensive further work will be required, we can consider two main characteristics previously reported.¹² The first is the sudden onset of plasticity after the shock front has propagated tens of unit cells which is reasonably temperature independent. For a particle velocity of 0.75 km s^{-1} in Cu-Mishin ($\sim 16\%$ compression), this distance is ~ 40 unit cells which would coincide with the modes falling on the unstable region if the mode locations are defined by the piston and the shock front.

The second is why we do not see all the $\{111\}$ slip planes populated with stacking faults for small cross sections in shock simulations. If we consider a system where only one mode lies in the unstable region then by symmetry there are four possible \mathbf{q} vectors that will grow exponentially, one in each of the four $\{111\}$ slip directions. If the unstable modes do not have initially equal populations then they will not reach critical amplitude at the same time. Once one set of planes have slipped, distorting the system, slippage in the other directions is likely to be inhibited. However, by making the simulation sufficiently large, sufficient inhomogeneity is introduced to allow nucleation of different planes in different regions which can then propagate throughout the system.

In summary, we have shown that the generation of stacking faults in MD simulations of perfect fcc crystals under uniaxial compression along [001] is due to the growth of soft phonon modes. As such, the time for defects to be generated is strongly temperature dependent, which is important in simulations of ramp-compressed fcc single crystals. The fact that the position in the BZ where the instability first occurs is not along a direction of high symmetry not only means that a conventional phonon-dispersion plot is inadequate but also that care must be taken when choosing the simulation box size. The implication is that this generation of stacking faults

is not something specific to shock simulations but instead is a fundamental instability of the lattice when uniaxially strained.

The authors would like to thank J. Belak, A. Higginbotham, W. J. Murphy, and B. Nagler for helpful discussions. G.K. is grateful for partial support for this work from LLNL under Subcontract No. B566832. P.E. and B.R. work under the auspices of the U.S. DOE by LLNL under Contract No. DE-AC52-07NA27344.

*justin.wark@physics.ox.ac.uk

- ¹S. Ogata, J. Li, and S. Yip, *Science* **298**, 807 (2002).
- ²G. Xu and A. S. Argon, *Mater. Sci. Eng., A* **319-321**, 144 (2001).
- ³D. Warner, W. Curtin, and S. Qu, *Nature Mater.* **6**, 876 (2007).
- ⁴C. L. Kelchner, S. J. Plimpton, and J. C. Hamilton, *Phys. Rev. B* **58**, 11085 (1998).
- ⁵R. E. Miller and A. Acharya, *J. Mech. Phys. Solids* **52**, 1507 (2004).
- ⁶J. Li, *MRS Bull.* **32**, 151 (2007).
- ⁷B. L. Holian, *Phys. Rev. A* **37**, 2562 (1988).
- ⁸P. A. Taylor and B. W. Dodson, *Phys. Rev. B* **42**, 1200 (1990).
- ⁹B. L. Holian, A. F. Voter, N. J. Wagner, R. J. Ravelo, S. P. Chen, W. G. Hoover, C. G. Hoover, J. E. Hammerberg, and T. D. Dontje, *Phys. Rev. A* **43**, 2655 (1991).
- ¹⁰V. V. Zhakhovskii, S. V. Zybin, K. Nishihara, and S. I. Anisimov, *Phys. Rev. Lett.* **83**, 1175 (1999).
- ¹¹B. Holian, J. Hammerberg, and P. Lomdahl, *J. Comput.-Aided Mater. Des.* **5**, 207 (1998).
- ¹²B. Holian and P. Lomdahl, *Science* **280**, 2085 (1998).
- ¹³T. C. Germann, B. L. Holian, P. S. Lomdahl, and R. Ravelo, *Phys. Rev. Lett.* **84**, 5351 (2000).
- ¹⁴J.-B. Maillet *et al.*, *Phys. Rev. E* **63**, 016121 (2000).
- ¹⁵D. Tanguy, M. Mareschal, P. S. Lomdahl, T. C. Germann, B. L. Holian, and R. Ravelo, *Phys. Rev. B* **68**, 144111 (2003).
- ¹⁶T. Germann *et al.*, *Metall. Mater. Trans. A* **35**, 2609 (2004).
- ¹⁷E. Bringa *et al.*, *J. Appl. Phys.* **96**, 3793 (2004).
- ¹⁸M. Shehadeh *et al.*, *Appl. Phys. Lett.* **89**, 171918 (2006).
- ¹⁹E. Bringa *et al.*, *Nature Mater.* **5**, 805 (2006).
- ²⁰B. Cao, E. Bringa, and M. Meyers, *Metall. Mater. Trans. A* **38**, 2681 (2007).
- ²¹M. A. Tschopp, D. E. Spearot, and D. L. McDowell, *Modell. Simul. Mater. Sci. Eng.* **15**, 693 (2007).
- ²²M. A. Tschopp and D. L. McDowell, *Appl. Phys. Lett.* **90**, 121916 (2007).
- ²³M. Meyers, *Scr. Metall.* **12**, 21 (1978).
- ²⁴D. M. Clatterbuck, C. R. Krenn, M. L. Cohen, and J. W. Morris, *Phys. Rev. Lett.* **91**, 135501 (2003).
- ²⁵J. Li *et al.*, *Mater. Sci. Eng., A* **365**, 25 (2004).
- ²⁶Y. Mishin, M. J. Mehl, D. A. Papaconstantopoulos, A. F. Voter, and J. D. Kress, *Phys. Rev. B* **63**, 224106 (2001).
- ²⁷S. Plimpton, *J. Comput. Phys.* **117**, 1 (1995).
- ²⁸Y. Mishin, D. Farkas, M. J. Mehl, and D. A. Papaconstantopoulos, *Phys. Rev. B* **59**, 3393 (1999).
- ²⁹P. Williams, Y. Mishin, and J. Hamilton, *Modell. Simul. Mater. Sci. Eng.* **14**, 817 (2006).
- ³⁰R. R. Zope and Y. Mishin, *Phys. Rev. B* **68**, 024102 (2003).
- ³¹F. Ercolessi and J. Adams, *Europhys. Lett.* **26**, 583 (1994).
- ³²E. C. Bain and N. Y. Dunkirk, *Trans. AIME* **70**, 25 (1924).
- ³³D. Wallace, *Thermodynamics of Crystals* (Dover, New York, 1972).